Association of marine viral and bacterial communities with reference black carbon particles under experimental conditions: an analysis with scanning electron, epifluorescence and confocal laser scanning microscopy

Fereidoun Rassoulzadegan, Markus G Weinbauer, Raffaela Cattaneo, Christian Rouviere

RESEARCH ARTICLE

Association of marine viral and bacterial communities with reference black carbon particles under experimental conditions: an analysis with scanning electron, epifluorescence and confocal laser scanning microscopy

Raffaela Cattaneo[1,2], Christian Rouviere[3], Fereidoun Rassoulzadegan[1,2] & Markus G. Weinbauer[1,2]

[1]Laboratoire d'Océanographie de Villefranche, Microbial Ecology & Biogeochemistry Group, Université Pierre et Marie Curie-Paris 6, Villefranche-sur-Mer, France; [2]Laboratoire d'Océanographie de Villefranche, CNRS-INSU, Villefranche-sur-Mer, France; and [3]Developmental Biology Unit, Université Pierre et Marie Curie-Paris 6, CNRS, Villefranche-sur-Mer, France

Correspondence: Markus G. Weinbauer, Laboratoire d'Océanographie de Villefranche, Microbial Ecology & Biogeochemistry Group, Université Pierre et Marie Curie-Paris 6, 06230 Villefranche-sur-Mer, France. Tel.: +43 49 376 3855; fax: +43 49 276 3834; e-mail: wein@obs-vlfr.fr

Received 25 June 2009; revised 30 April 2010; accepted 5 July 2010.
Final version published online 3 August 2010.

DOI:10.1111/j.1574-6941.2010.00953.x

Editor: Patricia Sobecky

Keywords
black carbon; particles; TEM; CLSM;DGGE; 16S rRNA gene.

Abstract

Black carbon (BC), the product of incomplete combustion of fossil fuels and biomass, constitutes a significant fraction of the marine organic carbon pool. However, little is known about the possible interactions of BC and marine microorganisms. Here, we report the results of experiments using a standard reference BC material in high concentrations to investigate basic principles of the dynamics of natural bacterial and viral communities with BC particles. We assessed the attachment of viral and bacterial communities using scanning electron, epifluorescence and confocal laser scanning microscopy and shifts in bacterial community composition using 16S rRNA gene denaturing gradient gel electrophoresis (DGGE). In 24-h time-course experiments, BC particles showed a strong potential for absorbing viruses and bacteria. Total viral abundance was reduced, whereas total bacterial abundance was stimulated in the BC treatments. Viral and bacterial abundance on BC particles increased with particle size, whereas the abundances of BC-associated viruses and bacteria per square micrometer surface area decreased significantly with BC particle size. DGGE results suggested that BC has the potential to change bacterial community structure and favour phylotypes related to *Glaciecola* sp. Our study indicates that BC could influence processes mediated by bacteria and viruses in marine ecosystems.

Introduction

Organic matter in seawater is a complex mixture of compounds of diverse chemical composition, physical structure and reactivity. Organic matter is operationally separated by filter cut-offs into dissolved organic matter (DOM) and particulate organic matter (POM). Seawater is currently considered as diluted gel with gel-like structures that can be formed from DOM or polymer chains, hence bridging the DOM–POM continuum (Verdugo *et al.*, 2004). Photosynthetically fixed carbon flows through three main pathways in the pelagic marine food web: the grazing food chain, the microbial loop (including the viral shunt) and sinking flux (Azam, 1998). Bacterial consumption of DOM is a major pathway that supports higher trophic levels. On an average, one-half of primary production is channelled into the microbial loop (Azam *et al.*, 1983; Ducklow, 2000). Organic matter–bacteria interactions influence the major properties and patterns of pelagic ecosystems such as new production and nutrient dynamics, as well as affect microbial community composition and activities (Simon *et al.*, 2002; Grossart *et al.*, 2006). Organic matter not only serves as a source of carbon and nutrients for heterotrophic bacteria, but also provides surfaces for attachment (Nagata, 2008). In particular, bacterial processing of POM affects the vertical flux of organic carbon from the surface to the interior of the oceans (Simon *et al.*, 2002).

In the particulate fraction, several classes of particles have been described such as colloids, submicron particles, Coomassie-stained particles, 4′-6-diamidino-2-phenylindole

FEMS MICROBIOLOGY ECOLOGY

(DAPI)-stained particles (DAPI yellow particles, DYP), Alcian Blue- and SYBR Gold-stained particles (filter fluorescing particles, FFP), transparent exopolymeric particles (TEP) and larger aggregates (Simon *et al.*, 2002; Nagata, 2008; Samo *et al.*, 2008). These particles are characterized by different sizes and properties and can harbour dense bacterial communities; bacterial abundances can be one or two orders of magnitude higher than in surrounding waters (Herndl, 1988). Moreover, particles support high bacterial diversity and represent hotspots of biogeochemical transformations (Azam, 1998). Thus, clarifying the mechanistic basis and control of organic matter–bacteria interactions is fundamental for a better understanding of ecosystem processes and biogeochemical cycling in the ocean.

Viruses can cause significant bacterial mortality (Weinbauer, 2004) and are known to infect bacteria on organic aggregates such as marine snow (Proctor & Fuhrman, 1991). When viruses lyse a cell, the cell content and cell wall fragments are released into the DOM and detritus pool (Wilhelm & Suttle, 1999). Viral lysis may also play an important role in early stages of organic aggregate formation and promote the formation of sinking particles. For example, the addition of viral concentrates from the natural community can delay marine snow formation, probably by delaying a bloom of phytoplankton (Peduzzi & Weinbauer, 1993). Interestingly, while the final total suspended matter concentration was not affected in rolling table experiments, the algal flocs were larger and more stable in the virus-enriched treatments (Peduzzi & Weinbauer, 1993). In the absence of phytoplankton, the presence of viruses can delay aggregate formation or colonization of aggregates by bacteria (Malits & Weinbauer, 2009). With regard to the effect of particulate matter on viruses, it has been argued that organic aggregates can cause a decay in viral infectivity (Suttle & Chen, 1992) and could have an inhibitory effect on viral production (Brussaard *et al.*, 2005; Mari *et al.*, 2005). However, there is evidence that at least in early stages of aggregate colonization, phage production is enhanced (Riemann & Grossart, 2008). In a study on mucilage, it has been shown that viral abundances and the virus to bacteria ratio (VBR) were highest on mature and aged aggregates (Bongiorni *et al.*, 2007). Overall, viral ecology on particles represents a relatively unexplored area of aquatic microbial ecology (Weinbauer *et al.*, 2009).

Black carbon (BC) is a carbonaceous residue of incomplete combustion of fossil fuels and biomass (Goldberg, 1985). It exists as a continuum of compounds ranging from slightly charred material to highly condensed, refractory soot (Hedges *et al.*, 2000; Masiello, 2004; Forbes *et al.*, 2006) and contributes to the DOM as well as the POM pool (Mannino & Harvey, 2004; Flores-Cervantes *et al.*, 2009). All components of this continuum are high in carbon content, chemically heterogeneous and dominated by aromatic structures (Hammes *et al.*, 2007). BC enters marine systems via the atmosphere, rivers or coastal runoff (Forbes *et al.*, 2006). Because of the refractory nature, BC is a sink in the global carbon budget. BC can constitute a significant fraction of organic carbon in seawater (Masiello & Druffel, 1998; Dittmar, 2008) and is also known to absorb very efficiently organic carbon (Cornelissen *et al.*, 2005). These features of BC suggest a role in organic matter cycling; however, its impact on marine ecosystems and microbial processes remains unknown.

The aim of this study was to investigate the short-term dynamics of BC particles and basic interactions between BC particles and a viral and bacterial community in marine coastal water. Using a standard reference BC, we examined the interaction of the bacterial and viral community in time-course experiments with BC using scanning electron microscopy (SEM), epifluorescence microscopy (EM) and confocal laser scanning microscopy (CLSM). We also assessed the potential of BC to change the community composition of bacterioplankton.

Materials and methods

Sampling and experimental set-up

Natural bacterial and viral communities from the marine plankton were used. Twenty-liter seawater samples were collected from surface water (*c.* 0.5 m depth) with a polycarbonate container (cleaned previously with 10% HCl) from the pier of the Laboratoire d'Océanographie de Villefranche (France; 43°41′47″N, 7°18′27″E). Experiment 1 (Exp1) was performed in fall (9 November 2007) and experiment 2 (Exp2) in summer (5 August 2008). *In situ* temperature and salinity profiles were recorded using a SEABIRD SBE25 CTD and obtained from the SOMLIT (Service d'Observation en Milieu LITtoral) monitoring program in the Bay of Villefranche.

To investigate experimentally the association of viruses and bacteria with BC, larger particles and most eukaryotes were removed by 0.8-μm filtration. Filtration was performed using acid-cleaned filtration units equipped with 47-mm-diameter polycarbonate filters (Nuclepore Track-Etch Membrane, Whatman) at approximately 100 mm Hg vacuum to avoid cell damage. Seawater, containing nominally only bacteria and viruses, was distributed in 500-mL acid cleaned glass flasks (Schott) and BC was added as powder at $10\,mg\,L^{-1}$. In all incubations, we used Diesel Particulate Matter (Industrial Forklift) Standard Reference Material (US National Institute of Standards and Technology, Department of Commerce,) as reference BC material. BC was mixed into the seawater by repeated gentle inversion of the bottles. Samples without BC were used as controls. Incubations were performed in triplicates at *in situ* temperature in

the dark. All treatments were maintained under turbulent conditions with a horizontal shaker set at 70 r.p.m. (IKA Labortechnik, KS 501 digitel). Experiments lasted for several days; however, most data (except some data on fingerprints; see below DNA extraction, PCR, community analysis and sequencing) are from the first 24 h.

Analysis of BC standard material

The carbon, hydrogen and nitrogen content of BC standard material was analyzed with a CHN analyzer (Perkin Elmer 2400) (Guieu *et al.*, 2005). The size distribution was analyzed with a Coulter Counter (Beckman Coulter Counter, Multisizer 3) in a flow of 0.2 μm filtered aged seawater. A sample of BC standard material was added at a final concentration of 10 mg L^{-1} to ultrapure water (Milli-Q, Millipore) and was analyzed using three different probes (30, 50 and 100-μm aperture tubes) (Yentsch & Yentsch, 2008).

Organic carbon

Samples for dissolved organic carbon (DOC) and total organic carbon (TOC) were collected only in Exp2 at the start of the experiment and after 24 h. Samples for DOC were filtered through precombusted (> 4 h at 450 °C) GFF filters (25 mm, Whatman) with a 25-mL glass syringe (Gastig 1025, Hamilton). The DOC and TOC concentrations were determined by high-temperature oxidation with a Shimadzu Total Organic Carbon-V CPH Analyser (Benner & Strom, 1993).

Microscopy

Samples for EM and CLSM were taken in 3–6-h intervals (until $T_{24\,h}$) and samples for SEM at only $T_{24\,h}$. The samples were fixed with glutaraldehyde (0.5% final concentration) for 15 min at 4 °C, shock-frozen in liquid nitrogen and stored at − 80 °C.

For SEM, samples (2 mL) were thawed, filtered at < 200 mm Hg vacuum pressure onto 0.02-μm pore size AlO_3 filters (25 mm diameter, Anodisc, Whatman) and dried at room temperature. To avoid interference from the membrane, samples were coated with evaporated carbon. Samples were investigated with a field emission scanning electron microscope (FESEM; JEOL 6700F) operated at 1.0 kV. Images were acquired by applying different detection modes: secondary electron image (SEI), lower secondary electron image (LEI) and backscattering electron detector (YAG).

For counting viruses and bacteria, slides for EM and CLSM were prepared using a slight modification of the Noble & Fuhrman method (1998). Briefly, particles from 2-mL samples were collected onto 0.02-μm pore size AlO_3 filters (25 mm diameter, Anodisc, Whatman) by low-pressure filtration and stained with SYBR Gold (Molecular Probes Inc., Eugene) at a 1000-fold dilution in autoclaved and 0.2-μm filtered ultrapure water. Filters were mounted on a glass slide with antifade mounting solution, i.e. *p*-phenylendiamine (final concentration, 0.1%; prepared freshly from a frozen 10% aqueous stock; Sigma-Aldrich, P-1519) in a Vectashield (Vector Laboratories) and Citifluor (Citifluor Ltd) solution (1 : 6, v : v). The slides were stored at − 20 °C until analysis.

Free-living and BC-associated viruses and bacteria were counted with an EM (Axiophot, Carl Zeiss) at × 1250 magnification similar to the method described by Luef *et al.* (2007). For free-living and BC-associated communities, at least 250 bacteria and viruses were counted on the same microscopic field; at least 20 fields were inspected. BC particles could be easily identified and stained viruses and bacteria were easily distinguished. Typically, we observed little or no background staining of BC particles. To confirm that viruses and bacteria were associated with BC, particles were inspected simultaneously in transmission light and epifluorescence mode. The VBR was calculated for BC-associated and free-living communities. EM was also used to assess the percentage of particles with associated viruses and bacteria.

The abundance of viruses and bacteria in relation to particle size and surface area was assessed with a CLSM (Leica SP2) equipped with an argon neon laser (excitation: 488 nm; emission spectrum: 530–550 nm). It has been shown before that viruses can be counted by CLSM on organic aggregates (Luef *et al.*, 2009a, b). First, slides were inspected manually in the epifluorescence mode, and viruses and bacteria associated with BC particles were enumerated at × 630 magnification. Then, for each particle, stacks of images were acquired alternatively in the light reflection and the epifluorescence mode to reconstruct the three-dimensional shape of the particle and the distribution of BC-associated viruses and bacteria (Fig. 1a–c). It is noteworthy that a manual definition is in general preferable to automated definition when assessing viruses with CLSM (Luef *et al.*, 2009a). The acquisition of images was optimized by adjusting the gain and offset on the photomultiplier to balance the intensity and background noise. The thickness of the acquisition field and the number of images per stack were defined manually depending on dimensions of the particles with the upper level corresponding to the top of the particles. The distance between consecutive images was *c.* 200 nm. Three-dimensional surfaces of BC particles were calculated using the IMAGE J application (http://rsb.info.nih.gov/ij/; version 1.5.0, NIH) from stacks of images acquired in the reflection mode. Because the laser cannot penetrate deep into BC particles (see Discussion), only the outer surface layer can be investigated and viruses and cells inside the particles cannot be detected. A macro was specially

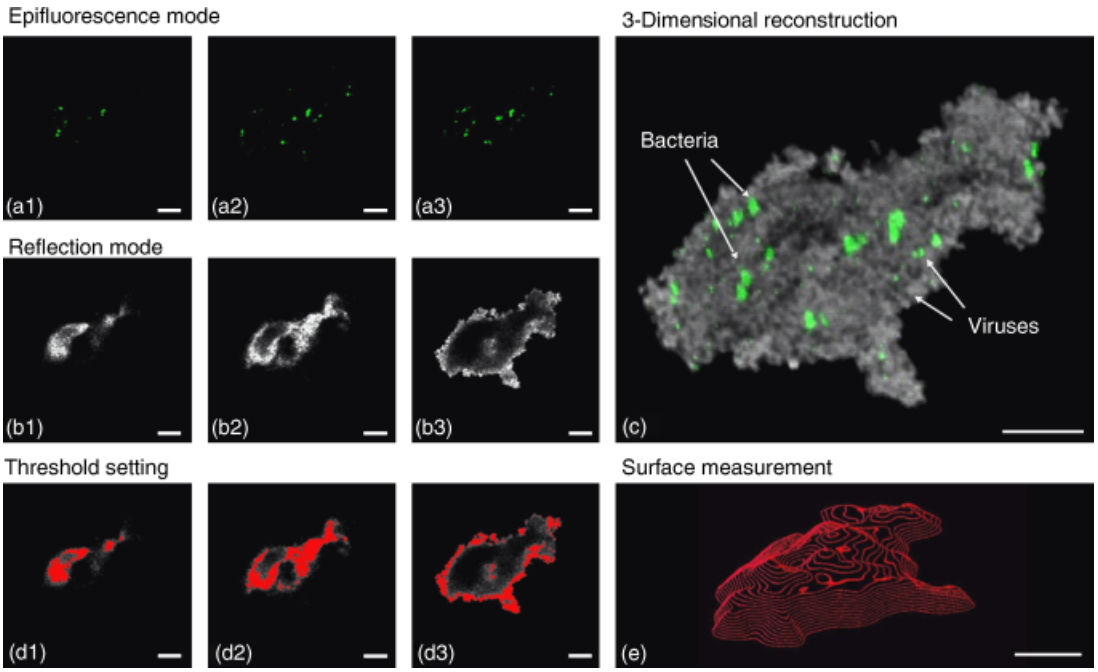

Fig. 1. CLSM image series of a BC aggregate. (a) (1–3) Images acquired in the epifluorescence mode. Viruses and bacteria are shown in green. (b) (1–3) Images acquired in the reflection mode. (c) Three-dimensional reconstruction obtained from integrated stacks. The arrows point to viruses and bacteria associated with the BC particle. (d) (1–3) Images from stacks acquired in reflection mode with manual settings of the threshold between light reflected by particles and background noise. Measured surfaces are shown in red. (e) Sum of selected areas and measurement of BC particle reconstructed by running a macro. Scale bar = 10 μm.

developed for this study to assess the surface area of BC particles. To run the macro, each image acquired on 256 gray scale was converted to a binary image, by distinguishing manually the background noise from BC particles (threshold setting, Fig. 1, D1–D3). Proceeding to the following image, the macro automatically measures surface areas of BC particles. The three-dimensional surface topology of the particle is given by the sum of all stepwise measurements (Fig. 1e). The operational mode is summarized in Fig. 1. The surface area of particles was converted into equivalent spherical diameter (ESD; i.e. the diameter of sphere with equivalent volume to nonspherical-shaped particles; Peduzzi & Weinbauer, 1993) using the following formula:

$$A = 4\pi r^2,$$

with A, surface area, and r, radius. At least 20 randomly selected particles per sample were investigated.

DNA extraction, PCR, community analysis and sequencing

At the end of Exp1 300-mL samples for bacterial community analysis were taken from control and BC treatments. Bacteria were collected first on 0.8-μm pore size filters and then bacteria in the filtrate were collected on 0.2-μm pore size polycarbonate filters (Cyclopore Track Etched Membrane; Whatman). These two fractions were operationally defined as particle-associated and free-living bacteria, respectively. During Exp2, no samples for bacterioplankton community composition were collected at $T_{24\,h}$. Instead samples from $T_{72\,h}$ are presented as a comparison.

DNA was extracted from the filters using a combination of four freeze–thaw cycles and enzymatic (proteinase K, lysozyme) digestion as described by Winter *et al.* (2001) and purified using a QIAEX II gel extraction kit (Qiagen) as recommended by the manufacturer. One microliter of DNA was used as a template for PCR amplification of a fragment of the bacterial 16S rRNA gene using the primer pair 341F-GC/907R (Schäfer & Muyzer, 2001). Conditions of the touchdown PCR were set as described in Schäfer & Muyzer (2001). PCR products were roughly quantified on 1.5% agarose gel electrophoresis by comparing band intensities with known amounts of a mass standard (Precision Molecular Mass Standard, Bioline) as described in Schäfer & Muyzer (2001).

Four hundred nanograms of PCR products were loaded on a denaturing gradient gel (30–70%) and run for 17 h using an INGENY phorU denaturing gradient gel electrophoresis (DGGE) system (Schäfer & Muyzer, 2001; Green, 2006). The gel was stained with SYBR Gold for 15 min in the

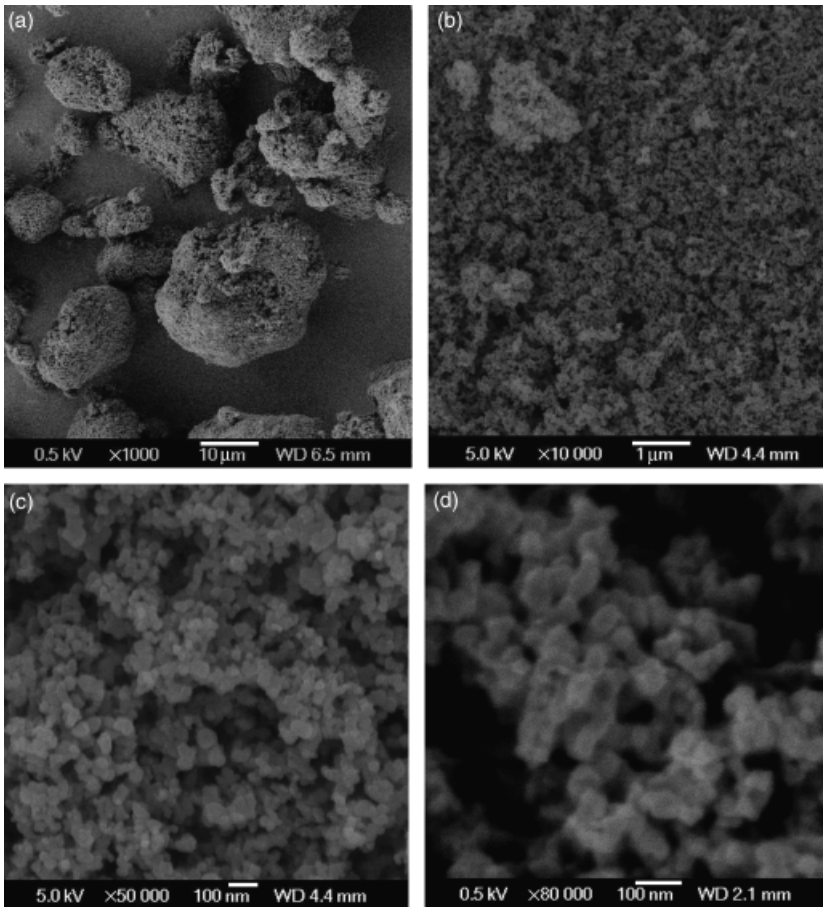

Fig. 2. SEM images of BC particles (untreated reference material). (a) × 1000, (b) × 10 000, (c) × 50 000, and (d) × 100 000 (detail of spherical units).

dark and visualized with the gel documentation system GelDoc EQ (Bio-Rad). Analysis of DGGE profiles was performed with QUANTITY ONE software (Bio-Rad).

For sequencing, selected bands were excised and eluted overnight in 20 µm sterile Milli-Q water and DNA was amplified as reported above using the 907R primer. DNA was sequenced by MWG-Biotech. Sequences were edited using the freeware program 4PEAKS 1.7 (A. Griekspoor and T. Groothuis, http://www.mekentosj.com) and a BLASTN search (http://blast.ncbi.nlm.nih.gov/Blast.cgi) was used to compare sequences against the GenBank no. database.

Statistical analysis

Mann–Whitney *U*-tests were used to assess differences of microbial parameters, organic carbon content and BC particle sizes between treatments, experiments and time points and performed with the software PRISM (GRAPHPAD). Nonparametric tests were used, because data did not show a normal distribution (even when transformations were used) and variances were typically not homogeneous. Relationships between microorganisms and particle parameters were assessed by correlation analysis after log transformation of data (Pearson correlation). A probability (P) of < 0.05 was considered significant. Cluster analyses of DGGE profiles were performed with QUANTITY ONE software (Bio-Rad) based on Ward's Dice coefficient.

Results

Reference BC material

The proportion of carbon, hydrogen and nitrogen of the Diesel Particulate Matter reference material was assessed, because this information is not included in the information leaflet from the supplier. Carbon represented $88.7 \pm 3.5\%$ of the weight of the material, while hydrogen and nitrogen constituted $0.9 \pm 0.1\%$ and $1.2 \pm 1.1\%$, respectively. BC particles ($25.2 \pm 3.4\%$) as detected by the Coulter Counter were smaller than 1.5 µm and more than $71.2 \pm 9.6\%$ were in the range between 1.5 and 4 µm ESD. Only $3.0 \pm 1.7\%$ of the particles were larger than 4 µm and $0.1 \pm 0.1\%$ of the particles were found in the size range between 10 and 30 µm.

An SEM electronmicrograph of relatively large BC particles is shown in Fig. 2. At the lowest used magnification (× 1000, Fig. 2a), particle sizes and shapes were variable. At

Table 1. *In situ* parameters at the time of water collection (0.5 m depth)

	Sampling dates	Temperature (°C)	Salinity (PSU)	Thermocline depth (m)	Viral abundance ($\times 10^6$ mL^{-1})	Bacterial abundance ($\times 10^5$ mL^{-1})	VBR
Exp1	November 9, 2007	17.7	38.1	70	14.2 ± 0.5	8.5 ± 0.6	16.7 ± 2.0
Exp2	August 5, 2008	24.5	38.2	20	10.3 ± 0.8	9.6 ± 1.7	11.0 ± 1.5

Values are averages ± SD of the means of three samples. Exp1, experiment 1; Exp2, experiment 2; PSU, practical salinity unit.

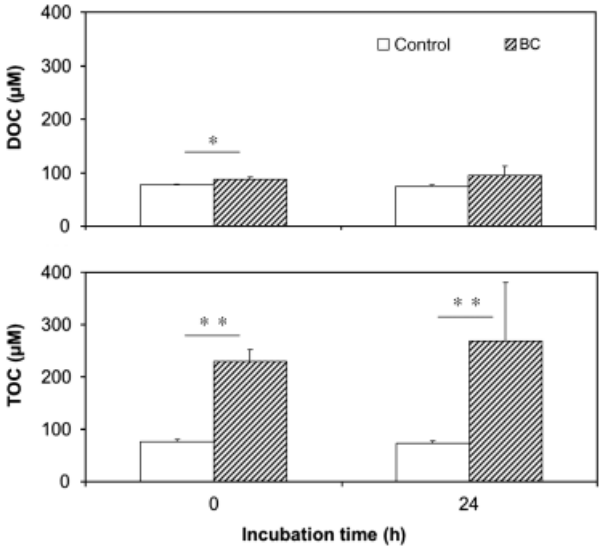

Fig. 3. Dynamics of DOC and TOC concentrations in BC and control treatments from Exp2. Values are given as averages ± SD of the means of triplicate incubations. $^*P < 0.05$; $^{**}P < 0.01$.

the micrometer scale, surfaces were extremely irregular. A × 10 000 magnification (Fig. 2b) showed that BC particles were composed of irregular aggregation of structural units, forming holes and protrusions. These units were spheres of 20–50 nm diameter (Fig. 2c and d).

In situ conditions

Water samples for experiments were collected in fall and in summer. In November, viral abundance and VBR were higher than in August, whereas temperature and bacterial abundance were lower. The water column was characterized by a deeper thermocline in August than in November (Table 1).

Organic carbon in experiments

Samples for DOC and TOC analyses were only collected in Exp2. The DOC concentration in the control did not change significantly during 24 h (average value, 75 ± 1.8 μM) (Fig. 3). Addition of BC caused an increase of DOC by 10 μM and of TOC by 155 μM. This difference in DOC between BC treatment and control was significant ($P < 0.05$). At $T_{24\,h}$, the DOC concentration was higher (by 21 μM) in the BC treatment than in the control but this difference was not significant ($P > 0.05$). At $T_{24\,h}$, the TOC concentration in the BC treatment was significantly higher (by 195 μM) than in the control ($P < 0.05$).

Using a carbon content of BC of 88.7%, 2.1 ± 0.3 mg L^{-1} BC could be recovered directly after addition of BC corresponding to 20.6 ± 2.8% of the added material. The fraction of BC in DOC was 6.5 ± 2.4% at $T_{0\,h}$. Assuming that the difference in carbon content between BC treatment and control at $T_{24\,h}$ is due to BC, 11.1 ± 7.7% of the BC was found in the DOC fraction and 2.6 ± 1.5 mg L^{-1} BC (or 25.9 ± 15.2%) of added material was recovered.

Effect of BC treatment on viral and bacterial abundance

In the controls, no attached viruses or bacteria were detected. At $T_{0\,h}$ of Exp1, 10.4 ± 1.0% of the viruses and 8.1 ± 1.6% of the bacteria were attached to BC particles (Table 2). In Exp2, 24.2 ± 1.7% of bacteria, 24.1 ± 0.3% of viruses were associated with particles at $T_{0\,h}$. Total detected viral abundance in the BC treatment at $T_{0\,h}$ was 73.9 ± 2.7% of the values in the control in Exp1 and 68.6 ± 6.1% in Exp2; corresponding values for bacteria were 65.9 ± 4.5% in Exp1 and 82.7 ± 10.5% in Exp2. Data obtained at $T_{12\,h}$ and $T_{24\,h}$ were typically not different (data not shown) and because other parameters such as DOC, TOC and DGGE were obtained only at $T_{24\,h}$, results were reported for this time frame.

During the incubation period (24 h), viral abundance in the controls decreased gradually by 13.2 ± 0.6% in Exp1 and by 3.1 ± 2.0% in Exp2 (Table 2); however, the difference between $T_{0\,h}$ and $T_{24\,h}$ was only significant for Exp1 ($P < 0.05$). In the BC treatments, the abundance of free-living viruses decreased by 82.2 ± 9.5% in Exp1 and 74.4 ± 4.7% in Exp2 and the difference between $T_{0\,h}$ and $T_{24\,h}$ was significant in both experiments ($P < 0.05$). In the BC treatments of both experiments, total viral abundance was significantly lower at $T_{24\,h}$ than at $T_{0\,h}$ ($P < 0.05$), whereas the abundance of BC-associated viruses was higher ($P < 0.05$). At the end of the experiments > 50% of the viruses were associated with BC particles and total viral abundance was significantly lower in the BC than in the control treatment ($P < 0.05$).

In the controls, bacterial abundance increased by 2.2-fold in Exp1 and 1.6-fold in Exp2. In both experiments,

Table 2. Microbial parameters at the start ($T_{0\,h}$) and at the end of the incubation period (after $T_{24\,h}$)

			Exp1			Exp2		
Time (h)	Treatment	Parameter	VA ($\times 10^6$ mL^{-1})	BA ($\times 10^5$ mL^{-1})	VBR	VA ($\times 10^6$ mL^{-1})	BA ($\times 10^5$ mL^{-1})	VBR
$T_{0\,h}$	CONTROL	Total	14.2 ± 0.5	8.5 ± 0.6	16.7 ± 2.0	10.3 ± 0.8	9.6 ± 1.7	11.0 ± 1.5
	BC	Free living	9.0 ± 1.1	4.6 ± 3.8	13.4 ± 1.5	5.4 ± 0.5	6.0 ± 0.7	9.0 ± 0.2
		Associated	1.1 ± 1.1	0.4 ± 0.3	11.8 ± 2.9	1.7 ± 0.1	1.9 ± 0.3	9.1 ± 1.2
		Total	10.5 ± 0.0	5.0 ± 4.1	13.2 ± 0.7	7.1 ± 0.6	7.9 ± 1.0	9.0 ± 0.5
$T_{24\,h}$	CONTROL	Total	12.3 ± 0.5	18.7 ± 5.7	6.9 ± 1.8	10.0 ± 0.9	15.5 ± 1.6	6.5 ± 0.1
	BC	Free living	2.6 ± 1.2	7.3 ± 1.3	3.4 ± 1.7	1.7 ± 0.1	11.1 ± 0.8	1.6 ± 0.2
		Associated	4.6 ± 0.8	9.0 ± 0.2	4.5 ± 0.2	3.0 ± 0.3	7.5 ± 0.3	4.0 ± 0.5
		Total	7.2 ± 1.6	16.4 ± 1.5	4.1 ± 0.8	4.7 ± 0.3	18.6 ± 0.8	2.5 ± 0.3

Values are averages $\pm$ SD of the means of triplicate incubations. Exp1, experiment 1; Exp2, experiment 2; VA, viral abundance; BA, bacterial abundance.

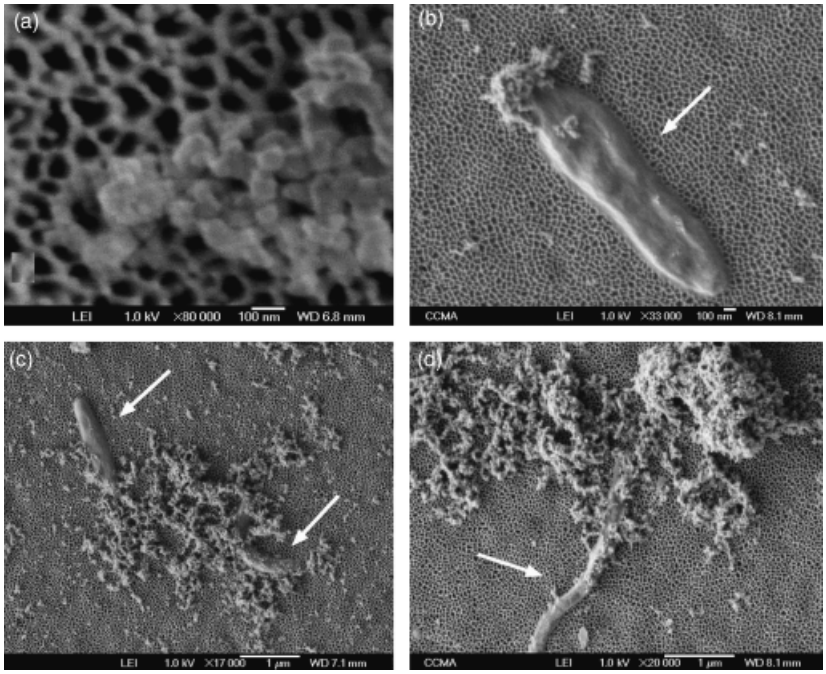

Fig. 4. SEM images of BC particles and bacteria collected onto an Anodisc filter after incubation in seawater. (a) $\times 80\,000$ (detail of spherical units), (b) $\times 33\,000$, (c) $\times 17\,000$, (d) $\times 40\,000$. (b–d) Interactions of BC and bacteria. The arrows point to bacterial cells.

free-living, BC-associated and, thus, total bacterial abundance in the BC treatment was significantly higher at $T_{24\,h}$ than at $T_{0\,h}$ ($P < 0.05$). At $T_{24\,h}$, total bacterial abundance in the BC treatments was not significantly different from the controls in Exp1 but significantly higher in Exp2 ($P < 0.05$). At $T_{24\,h}$, $55.4 \pm 4.1\%$ of the bacteria were associated with BC particles in Exp1 compared with $40.4 \pm 2.3\%$ in Exp2.

In the control, VBR decreased from 16.7 ± 2.0 at $T_{0\,h}$ in Exp1 and 11.0 ± 1.5 in Exp2 to 6.9 ± 1.9 and $6.5 + 0.1$ in Exp1 and Exp2, respectively at $T_{24\,h}$ (Table 2). In the BC treatment of Exp1, VBR decreased from 13.4 ± 1.5 at $T_{0\,h}$ to 3.9 ± 1.7 at $T_{24\,h}$ for the free-living community and from 11.8 ± 2.9 at $T_{0\,h}$ to 4.5 ± 0.2 at $T_{24\,h}$ for the BC-associated community. In Exp2, VBR in the BC treatment decreased from 9.0 ± 0.2 at $T_{0\,h}$ to 1.6 ± 0.2 at $T_{24\,h}$ for the free-living community; values for BC-associated communities were 9.1 ± 1.2 and 4.0 ± 0.5, respectively. The differences between $T_{0\,h}$ and $T_{24\,h}$ were significant (always $P < 0.05$). At $T_{24\,h}$, VBR was higher for BC-associated than for free-living communities, but this difference was only significant for Exp2 ($P < 0.05$).

Detection of microorganisms on BC particles in experiments

SEM and CLSM inspection of samples with and without BC additions showed that there was no material in seawater detectable in quantities that could be confounded with BC standard material. Thus, BC particles could be easily identified in the experimental treatments. SEM inspection suggests that the elementary structures of BC, i.e. the spherical units, were not modified by incubation in seawater (compare Figs 2 and 4). However, in seawater, BC particles appeared less rigid in the sense of showing less coherence

or even falling apart compared with reference material not exposed to seawater. Figure 4 also indicates that BC spherical units or very small BC particles can attach to bacterial cells.

Bacteria associated with BC could be detected using SEM, while no viruses could be clearly identified. Bacteria were associated with or trapped within BC particles (Figs 4 and 5); also, colloidal BC seemed to be associated with bacteria (Fig. 4b). The image in Fig. 5a shows that BC-associated bacteria were not easily detectable using the LEI detection mode. However, using other detectors on the same filter field (Fig. 5) improved the detection of BC-associated bacteria. Using the SEI detector, BC particles were not clearly visible, but bacterial cells appeared as distinct areas (Fig. 5b). In contrast, structures of BC particles were identified better with the LEI detector (Fig. 5a). The YAG detector provided the best combined resolution for bacteria and particles together with a lower resolution for bacteria than the SEI detector and a lower resolution for BC particles than the LEI detector (Fig. 5c).

A three-dimensional reconstruction of a particle with associated microorganisms is shown in Fig. 1. Stacks of images acquired in the reflection mode by CLSM revealed a highly irregular shape of BC particles. Images acquired in the epifluorescence and the reflection mode showed the actual distribution of viruses and bacteria on the particles.

In order to test whether free-living viruses and bacteria were collected onto particles during filtration, thus producing colonized particles, the following test was performed. Particles were added to 2 mL ultrapure water at a final concentration of 10 mg L^{-1} and filtered onto the Anodisc filter. Successively, 2 mL seawater containing SYBRGold was filtered onto the same filter. No viruses were observed on BC particles and on $0.5 \pm 0.1\%$ of the particles bacteria (max 2) were observed. This suggests that collection of viruses and bacteria onto particles during the filtration process did not create a significant bias of microbial abundances on particles.

Relationship of microorganisms with BC particles in experiments

EM counts showed that microorganisms were associated with $37.1 \pm 6.7\%$ of BC particles in Exp1 compared with $40.1 \pm 5.0\%$ in Exp2. In the following, only particles with associated viruses and bacteria are considered. The number of particles was in the order of magnitude of 10^5 m L^{-1}.

The size of BC particles with associated viruses and bacteria varied between 2.4 and 52.5 μm ESD in Exp1 and between 4.0 and 20.1 μm ESD in Exp2. Particles smaller than 5 μm ESD represented on average $4.9 \pm 3.5\%$ in Exp1and $4.4 \pm 4.0\%$ Exp2 (Fig. 6a). Particles in the size range between 5 and 10 μm averaged $38.7 \pm 15.9\%$ of total particle counts in Exp1 and $70.2 \pm 5.1\%$ in Exp2. Finally, particles larger

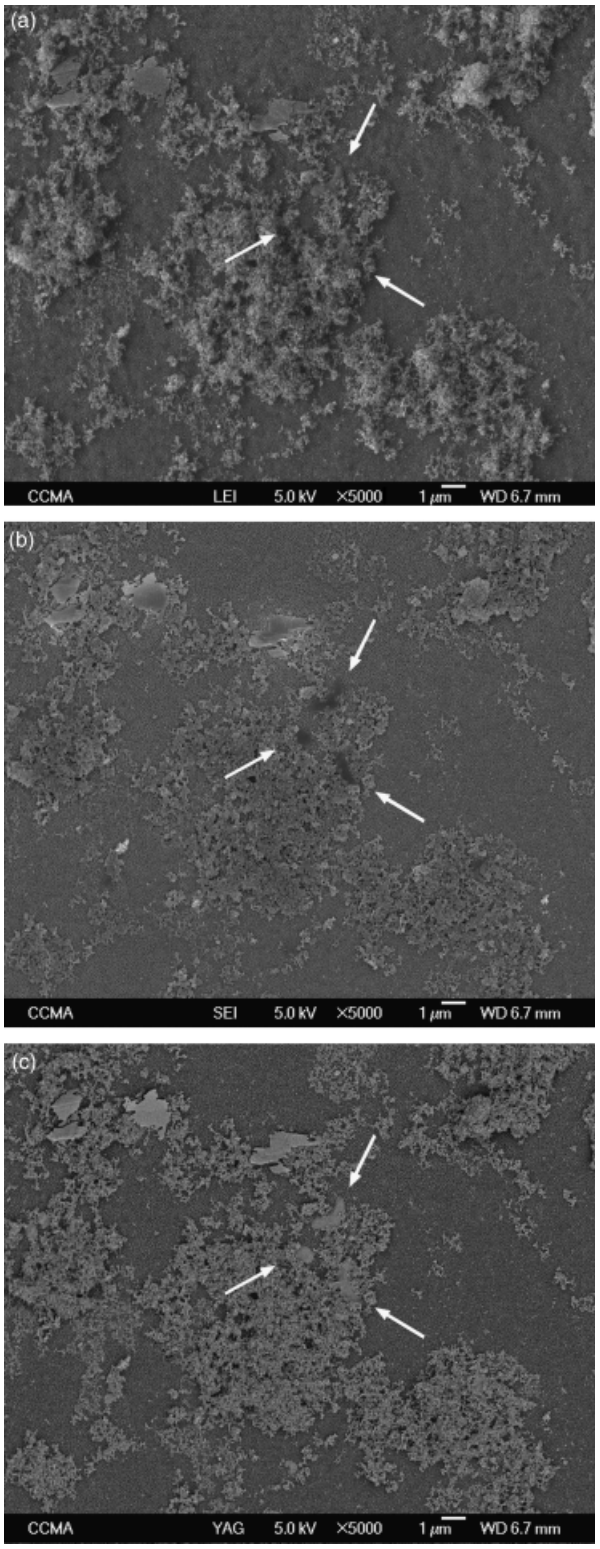

Fig. 5. SEM images obtained in different detection modes. (a) Lower secondary electrons image, detector LEI; (b) secondary electrons image, detector SEI; (c) backscattered electrons image, detector YAG. The arrows point to bacterial cells.

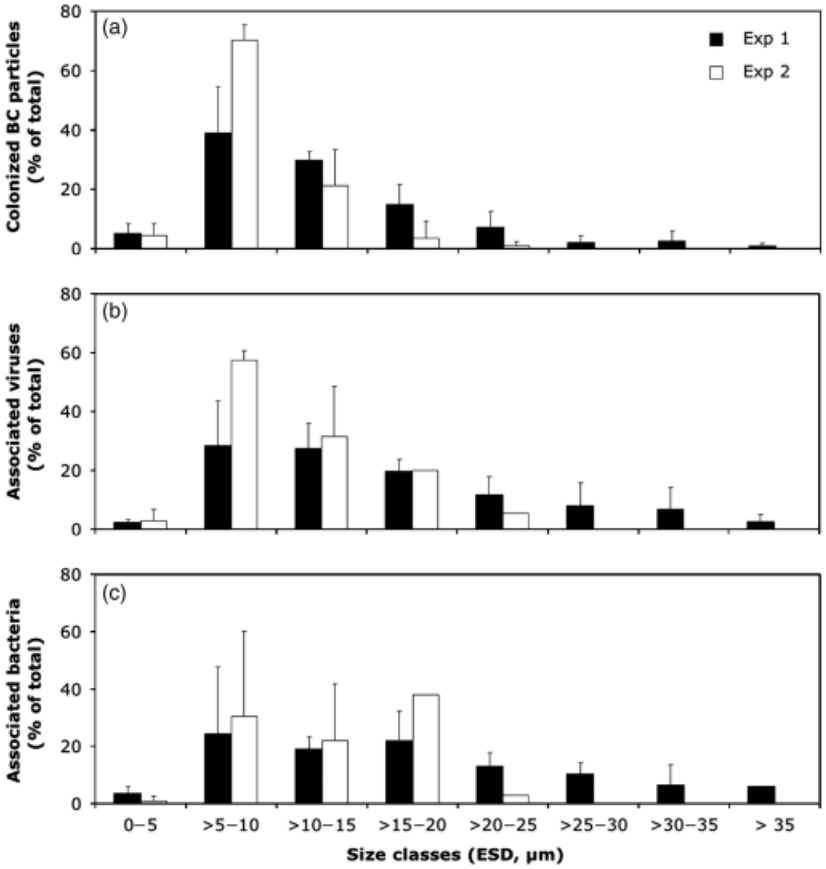

Fig. 6. Size class distribution of the percentage of BC particles with both associated viruses and bacteria (a) and contribution of BC-associated viruses (b) and bacteria (c) to the total abundance in the different BC particle size classes. Exp1, experiment 1; Exp2, experiment 2; ESD, equivalent spherical diameter. Values are given as averages ± SD of the means of triplicate incubations.

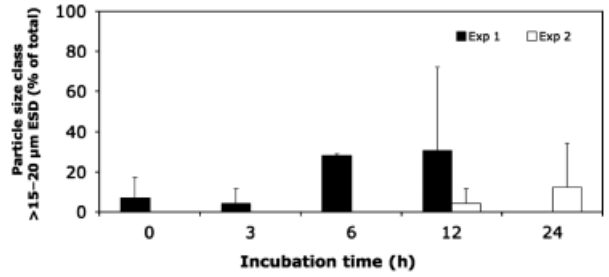

Fig. 7. Temporal changes of the percentage of BC particles with associated viruses and bacteria in the size class > 15–20 µm. Exp1, experiment 1; Exp2, experiment 2; ESD, equivalent spherical diameter. Values are given as averages ± SD of the means of triplicate incubations.

than 20 µm contributed 11.7 ± 13.2% in Exp1 and 0.9 ± 1.5% in Exp2.

The average particle size (*c.* 10 µm ESD) did not vary significantly between sampling time points of the experiments and did not differ significantly between corresponding time points of the two experiments (always $P > 0.05$) (data not shown). However, significant differences between time points were found for the relative contribution of several size classes of particles ($P < 0.05$). For example (Fig. 7) in Exp1, the particle size class > 15–20 µm represented 7.1 ± 10.1% of total particles immediately after BC addition and did not differ significantly at $T_{3\,h}$, $T_{6\,h}$ and $T_{12\,h}$ ($P > 0.05$). After 24 h incubation, no particles were found in this size class. In Exp2, no particles were detected in the size class > 15–20 µm at $T_{0\,h}$, $T_{3\,h}$ and $T_{6\,h}$. Between $T_{12\,h}$ and $T_{24\,h}$, the contribution of particles in the size range of > 15–20 µm became detectable (4.2–13.5%).

The number of BC-associated viruses counted on individual BC particles varied between 2 and 340 in Exp1 and between 5 and 103 in Exp2. In Exp1, on 46.1 ± 14.2% of the particles between 10 and 40 viruses were detected, whereas in Exp2 this percentage was 67.9 ± 18.3%. In Exp1, on 15.9 ± 9.3% of the BC particles > 100 viruses were detected. In both experiments, most viruses (55.7 ± 23.2% of total BC-associated viruses in Exp1 and 88.7 ± 18.7% in Exp2) were found on particles between 5 and 15 µm ESD (Fig. 6b). A positive and significant correlation was found in both experiments between the abundance of BC-associated viruses per particle and BC particle size ($r = 0.49$, $P < 0.001$; Table 3). The number of BC-associated viruses per square micrometer surface of particles decreased significantly with increasing particle size ($r = -0.43$, $P < 0.001$; Table 3).

Particles with only bacteria and no viruses were not observed in the two experiments. In Exp1, both viruses and bacteria were associated with only 50.8 ± 16.3%; for Exp2

Table 3. Correlation analysis of microbial abundances with particle parameters (Pearson's correlation)

	Exp 1			Exp 2		
	r	*n*	*P*	*r*	*n*	*P*
Abundance of attached viruses vs. BC particle size	0.49	464	< **0.001**	0.62	108	< **0.001**
Abundance of attached bacteria vs. BC particle size	0.13	154	NS	0.57	74	< **0.001**
VBR vs. BC particle size	0.27	154	< **0.01**	−0.08	74	NS
Abundance of attached viruses per square micrometer vs. BC particle size	−0.43	464	< **0.001**	−0.44	108	< **0.001**
Abundance of attached bacteria per square micrometer vs. BC particle size	−0.32	154	< **0.01**	−0.41	74	< **0.001**
VBR per square micrometer vs. BC particle size	−0.40	154	< **0.001**	−0.50	74	< **0.001**

Significant values are shown in bold. Exp1, experiment 1; Exp2, experiment 2;NS, nonsignificant.

this contribution was 70.7 ± 13.4%. In Exp1, up to 59 bacteria were found on BC individual particles, whereas not more than 10 bacteria were counted on BC particles in Exp2. Between 55% and 61% of the particles colonized by bacteria were only colonized by one to two bacterial cells. The percentage of BC-associated bacteria on total bacteria was highest (*c.* 65% in both experiments) in the particle size range > 5–20 μm (Fig. 6c). A significant correlation between the abundance of BC-associated bacteria and the size of BC particles was only found in Exp1; however, the correlation coefficient was also positive in Exp2 ($r = 0.57$, $P < 0.001$; Table 3). The abundance of BC-associated bacteria per square micrometer particle surface decreased significantly with particle size in both experiments ($r = -0.32$, $P < 0.01$).

The VBR on BC particles ranged from 0.2 to 154.0 in Exp1 and from 4.6 to 63.0 in Exp2. In Exp1 > 70% of the values showed ratios between 10.0 and 90.0. The VBR was positively correlated ($r = 0.27$, $P < 0.01$) with BC particle size in Exp1, whereas no significant correlation was found in Exp2 (Table 3). In both experiments, VBR per square micrometer particle surface increased significantly ($r = -0.4$, $P < 0.001$) with BC particle size.

Changes of bacterial community composition

In neither of the two experiments could bacterial PCR products be obtained from the 0.8-μm filters, whereas bacterial PCR products could be obtained from the 0.2-μm filters. In Exp1, eight bands were detected; six to seven bands were found in the control and all eight in the BC treatment. Seven bands were shared between control and BC treatment, and one band was specific for the BC treatment. A cluster analysis showed that bacterial fingerprints clearly differed between the control and the BC treatment with a similarity of 70% (Fig. 8). In Exp2, nine different DGGE bands were detected. Seven bands were found in the control and eight in the BC treatment. Two bands were specific for the BC treatment and one for the control. Six bands were shared between control and BC treatment. A cluster analysis showed that the bacterial fingerprints differed between the BC treatment and the control; overall similarity was 40% (Fig. 8).

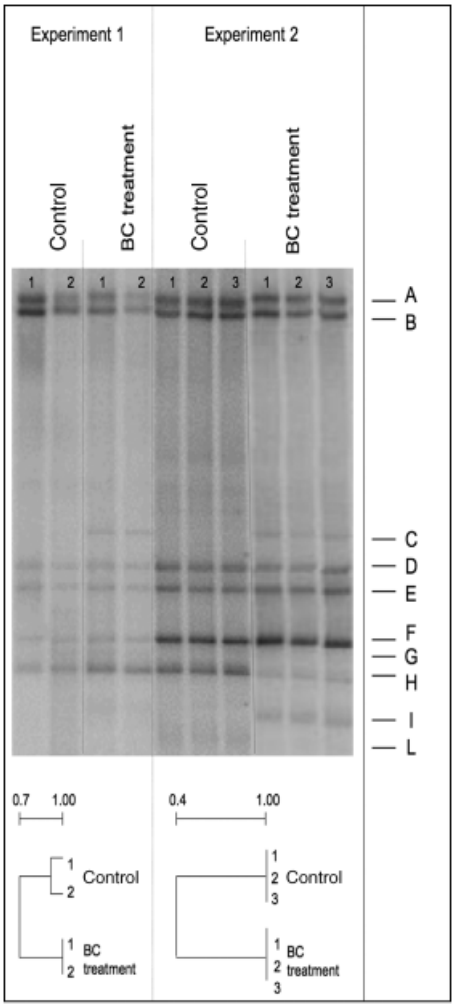

Fig. 8. DGGE gels and cluster analysis of bacterial community composition in the experiments. Letters refer to sequenced bands (Table 4). The cluster analysis is given as a fraction of similarity. In Exp1, only filters from two replicates were analysed.

The results of the sequencing of bands are summarized in Table 4. The band L, which was only present in the control of

Table 4. Phylogenetic affiliation of sequences from DGGE bands with closest uncultured matches

Band identity	Closest match	GenBank accession no.	Sequence similarity in % (no. of bases)	Taxonomic group
A	Uncultured *Rhodobacteraceae* clone TDNP	FJ516768	87 (475)	*Alphaproteobacteria*
B	Uncultured *Ruegeria* sp. clone pltb-RF-3	AB294982	97 (461)	*Alphaproteobacteria*
C	Uncultured *Glaciecola* sp. clone D1544	EU258751.1	100 (474)	*Gammaproteobacteria*
D	Uncultured *Rhodobacteraceae* bacterium clone SHWN_night2	FJ745271.1	100 (497)	*Alphaproteobacteria*
E	Uncultured *Ruegeria* sp. clone SIMO-846	AY712383.1	94 (474)	*Alphaproteobacteria*
F	Uncultured *Rhodobacteraceae* bacterium clone SHWN_night2	FJ745271.1	100 (485)	*Alphaproteobacteria*
G	Uncultured *Ruegeria* sp. clone SIMO-428	AY711965	100 (470)	*Alphaproteobacteria*
H	Uncultured *Rhodobacteraceae* bacterium clone 2_B6	EU600598.1	100 (466)	*Alphaproteobacteria*
I	Uncultured *Glaciecola* sp. clone D1544	EU258751.1	100 (493)	*Gammaproteobacteria*
L	Uncultured gamma proteobacterium clone 2_B1	EU600670.1	96 (479)	*Gammaproteobacteria*

The number of bases used to calculate sequence similarity is in parenthesis in the fourth column. The *E*-value was 0.0 for all bands except for band A (*E*-value, 8e-146).

Exp2, showed the closest sequence similarity (96%) to an uncultured *Gammaproteobacteria* clone. The two bands (C and I) exclusively found in BC treatments were 100% identical to an uncultured clone of the genus *Glaciecola*. One band (H), with a sequence most closely related to an uncultured *Rhodobacteriaceae* clone, showed a higher relative band intensity in the control than in the BC treatment in Exp2 but not in Exp1.

Discussion

Methodological considerations and evaluation of experimental approach

Our study as conducted using BC reference material. BC is variable in chemical and biological reactivity (Hedges *et al.*, 2000; Hammes *et al.*, 2007), and thus, could differ from reference material. Nevertheless, the use of reference material allows for controlled and repeatable experimental conditions. In addition, the general elementary structures of the Diesel reference material were spherical (Fig. 2), and thus, coherent with the model of onion-type particles proposed by Schmidt & Noack (2000). Analysis of dry BC material by SEM allowed assessment of the structure and morphological properties of BC as it is emitted from sources. Also, BC from Diesel fuel can be a significant portion of BC found in marine systems (Novakov *et al.*, 2000; Aymoz *et al.*, 2007; Sandradewi *et al.*, 2008).

BC concentrations added ($10\,mg\,L^{-1}$) were higher than the maximum value of $162\,\mu g\,BC\,L^{-1}$ found in the ultrafiltered DOM fraction of coastal seawater (Mannino & Harvey, 2004). The range of 135–$288\,\mu g\,BC\,L^{-1}$ found in the DOC fraction of our study is similar to this value. However, we found in our experimental conditions with reference to BC material that the dissolved BC fraction was at maximum 11.1% of TOC. Thus, it is possible that previous studies (Masiello & Druffel, 1998; Mannino & Harvey, 2004) have missed some particulate BC. In the TOC fraction, recovered BC concentrations ranged from 2.1 to $2.6\,mg\,L^{-1}$ or 21–26% of added material. One of the reasons for the low BC concentrations detected could be that a fraction of the added BC became associated with the walls or settled to the bottom of the incubation bottles, as visible BC started to accumulate at the bottom of incubation flasks, although incubation flasks were agitated.

Several arguments can be put forward to support an experimental approach with high BC concentrations. (1) A quantitative investigation by CLSM requires a high number of BC particles. (2) Our study was rather targeted to study principle interactions between BC and microorganisms than simulating typical scenarios. (3) High BC concentrations can be expected on small temporal or spatial scales, for example when fly ash enters the water or at submersed exhaust pipes of boats (as reported by Mannino & Harvey, 2004).

No viral-like particles could be identified by SEM, neither associated with the BC particles nor from ambient water, i.e. on the filter surface. It is noteworthy that SEM is typically not used to identify viruses, and therefore, this result is not surprising. Bacteria could be easily identified by SEM on the filter but only with difficulties on the particles. Bacterial cells and BC particles responded in a different way to the electronic excitation. Thus, by operating at different detection modes on the same optical field, it is possible to distinguish between BC particles and the bacteria localized on them.

During the last decade, CLSM has been used to investigate the three-dimensional structure of biofilms and riverine and marine snow (Halloway & Cowen, 1997; Beyenal *et al.;* 2004; Neu *et al.*, 2004). In recent studies, CLSM has been applied to visualize the distribution of viruses and bacteria in river particles (Luef *et al.*, 2009a, b). In our study, CLSM has been used to investigate interactions between BC particles and marine viruses and bacteria. In agreement with

the finding of Luef *et al.* (2009a) for riverine particles, we found that automated detection of viruses on BC particles is not yet possible by CLSM. Therefore, viruses (and bacteria) were counted manually. As for other organic particles (Luef *et al.*, 2007; Peduzzi & Luef, 2008), the penetration depths of CLSM or EM into BC particles is limited. Thus, we could not assess microbial abundance deep inside the particles or on the backside of particles. This should have resulted in an underestimation of microbial abundance, for example if colonized particles had aggregated and trapped viruses and cells inside. This could explain the lower total viral and bacterial abundance in the BC treatment compared with the control at $T_{0\,h}$, although we cannot fully exclude the possibility that this difference was due to sinking of particles or attachment of particles to the walls of the incubation flasks (see discussion above on BC recovery). An underestimation of viral and bacterial abundance on particles could particularly play a role for larger particles (because the surface to volume ratio decreases with particle size) and explain why we did not always find a relationship between microbial abundance and particle size.

Dynamics of BC particles

We found statistically significant changes of the size distribution of BC particles within 24 h and that this pattern differed between the two performed experiments (Fig. 7). Dissolution or disaggregation of particles by enzymes is possible, because it is known that exoenzymes produced by associated bacteria can dissolve organic aggregates (Smith *et al.*, 1992; Kepkay, 1994; Azam & Long, 2001). Nevertheless, aggregation and disaggregation processes driven by factors such as variations in temperature, organic matter load and productivity seem more likely responsible for the change of particle size. BC-like chemicals such as activated charcoal are well-known absorbents of organic matter (Busscher *et al.*, 2008), and in our study, viruses and bacteria became associated with BC particles. In the bay of Villefranche, seasonal variations of environmental parameters can play an important role in the dynamics of DYP (Mostajir *et al.*, 1995) and the aggregation of TEP (Beauvais *et al.*, 2003). DYP concentrations are typically higher in November than in August (Mostajir *et al.*, 1995), whereas TEP concentrations are lower (Beauvais *et al.*, 2003). Thus, it is also possible that interactions with different types of particles influenced the aggregation of BC particles.

Microorganism–particle interactions and relationship with particle size

Interestingly, in one of our experiments, VBR increased with particle size, whereas a negative relationship was found for riverine aggregates (Luef *et al.*, 2007). In addition, VBR was higher in the BC-associated than in the free-living microbial communities (Table 2), whereas the VBR was lower on floating particles than in ambient water in riverine system (Luef *et al.*, 2007). The high VBR and viral abundances on BC particles at $T_{24\,h}$ and the increase of these parameters with particle size could be due to several reasons. For example, the high values could be the result of a higher attachment rate to BC particles for viruses. An experimental study with a phage–host system reported on high VBR values on colonized agar spheres and interpreted that as elevated particle-associated phage production probably due to enhanced encounter rates (Riemann & Grossart, 2008). It has also been shown that aromatic hydrocarbons can induce phage production in lysogenic bacterial communities (Cochran *et al.*, 1998). However, in contrast to these studies, we found a reduction of total viral abundance due to BC additions. Thus, it is more likely that viruses were more rapidly associated with BC particles than bacteria.

The number of BC-associated viruses and bacteria per square micrometer was negatively correlated to BC particle size as reported in previous studies on other suspended material (Simon *et al.*, 2002; Luef *et al.*, 2007). Also, the volume-specific abundance of viruses on TEP decreased with TEP size (Mari *et al.*, 2007). For organic aggregates *in situ*, this might be due to ageing of particles, where reduced organic matter bioavailability could reduce production of bacteria and viruses. However, this cannot be the cause in our short-term incubations. One explanation could be that larger particles have a different three-dimensional composition than smaller particles. For example, the shear applied could make the particles more porous. A higher porosity would mean a larger percentage of pore water with lower microbial abundances. This could explain the lower microbial abundance per surface area in larger particles. Moreover, because BC particles are typically fractal (Slowik *et al.*, 2007), a change of particle size can correspond to a change of porosity (Logan & Wilkinson, 1990). A change of viral and bacterial density could then be linked to fractal dimension, i.e. the porosity of the particles.

Effect of BC on bacterial community composition

We did not obtain a bacterial PCR product from DNA extracted from 0.8-μm filters. For the controls, this suggests a low fraction of particle-associated bacteria. Because a large portion of bacteria was associated with BC particles in the experiments (Table 2; note that in Exp2 the percentage of attached bacteria was not significantly different between $T_{24\,h}$ and $T_{72\,h}$; data not shown), this could suggest that DNA extraction or PCR amplification was inhibited by BC. Alternatively, breakage of BC particles during filtration could have released bacteria into the free-living fraction. Thus, we do not have information of the bacterial

community composition of BC-associated bacteria. However, the addition of BC induced changes of community composition of free-living bacteria. This could be due to changes in viral pressure as a result of viral attachment. For example, if specific viral types become associated in different rates, this could change viral infection and lysis of specific phylotypes, and thus, affect community structure. Because BC readily absorbs organic matter (Busscher *et al.*, 2008), the organic matter field could be changed by BC, for example by creating hot spots of organic matter transformation. Such a mechanism could also influence the free-living community. Another cause could be direct antagonistic or stimulating effects of BC. Among antagonistic effects could be attachment of BC to bacteria or trapping of bacteria in BC (Figs 4 and 5) and, for example, reduced uptake of nutrients. The two phylotypes corresponding to the genus *Glaciecola* were only detected in the BC treatment (at $T_{24\,h}$ of Exp1 and $T_{72\,h}$ of Exp2). The genus *Glaciecola*, which is phylogenetically closely related to the genus *Alteromonas* (Bowman *et al.*, 1998), consists of facultative oligotrophic chemoheterotrophs (Van Trappen *et al.*, 2004). This could indicate a metabolic skill to mineralize complex organic compounds such as BC, for example production of mono- or dioxygenases (Brakstad *et al.*, 2008). Interestingly, a recent study on the effect of crude oil petroleum on the bacterial community in Arctic Sea ice showed a change in community composition with an increased abundance of few genera including *Glaciecola* (Brakstad *et al.*, 2008). Addition of BC, which shares with oil the aromatic structure, could have favoured the growth of bacteria from the genus *Glaciecola* with hydrocarbon biodegradation skills. While the appearance of *Glaciecola*-related phylotypes could be due to the high BC concentrations used, we have also identified a potential candidate for BC degradation. Assuming that *Glaciecola*-related phylotypes indeed used BC, our findings could suggest that the free-living community used dissolved or very small particulate BC. Although we have only information on the community composition of free-living bacteria, our data indicate that BC has the potential to affect the community composition of bacterioplankton.

Implications and future research directions

The attachment of viruses could have inactivated viruses, i.e. irreversibly destroyed infectivity, or prevented infection of bacteria because of the morphology of BC particles. For example, attachment of BC to bacteria such as indicated in Fig. 4 could block or hide receptor sites for viral attachment. This could explain the reduction of total and free-living viral abundance and VBR found in our study. A reduction of viral abundance should relieve the viral pressure and decrease virus-induced mortality of bacteria. Indeed, addition of BC stimulated bacterial abundance in Exp2. Bacterial cells also seem to be trapped within BC particles (Figs 4 and 5). This could result in either a better availability of organic carbon or in problems with gas or matter exchange. Such open questions can be addressed in experimental studies with BC by assessing viral production, virus-mediated mortality of bacteria and bacterial production.

Although our data do not provide an in-depth analysis of community composition, they suggest that BC has the potential to influence bacterial diversity and favour specific phylotypes. The advent of relatively inexpensive large-scale sequencing approaches will allow in-depth testing of these hypotheses. We observed in our experiments sedimentation of BC particles. Thus, attachment and sinking could be a mechanism to transport viruses and bacteria to sediments and deep water layers. Several types of particles have been recognized, such as colloids, submicron particles, DSP, CYP, TEP, FFP or larger organic aggregates. BC is an additional type of particle not studied so far in aquatic microbial ecology.

The crucial role of anthropogenic BC for atmospheric processes such as global warming and the formation of the Asian brown cloud has been well-documented (Bond *et al.*, 2004; Ramanathan & Carmichael, 2008). As BC is deposited into the ocean (Forbes *et al.*, 2006) and seems to affect the microbial food web (this study), further research on BC effects on microbial processes such as the trophic balance, organic matter transport and bacteria-mediated assimilation of organic carbon and on microbial diversity in aquatic ecosystems is warranted.

Acknowledgements

This research was supported by the Eur-Oceans Network of Excellence (Project Number WP4-SYSMS-1021). The EM work was performed at the Centre Commun de Microscopie Appliqué (University of Nice, France). We thank Christian Griebler for suggestions and John Dolan for improving the English. Three anonymous reviewers improved the manuscript. SOMLIT is acknowledged for providing data on temperature and salinity. Some support was also provided by the projects ANR-AQUAPHAGE (No. ANR 07 BDIV 015-06) and ANR-MAORY (No. ANR 07 BLAN 016) from the French Science Ministry.

References

Aymoz G, Jaffrezo JL, Chapuis D, Cozic J & Maenhaut W (2007) Seasonal variation of PM10 main constituents in two valleys of the French Alps. I: EC/OC fractions. *Atmos Chem Phys* **7**: 661–675.

Azam F (1998) Microbial control of oceanic carbon flux: the plot thickens. *Science* **280**: 694–696.

Azam F & Long RA (2001) Sea snow microcosms. *Nature* **414**: 495–498.

Azam F, Fenchel T, Field JG, Gray JS, Meyer-Reil LA & Thingstad TF (1983) The ecological role of water-column microbes in the sea. *Mar Ecol-Prog Ser* **10**: 257–263.

Beauvais S, Pedrotti ML, Villa E & Lemee R (2003) Transparent exopolymer particle (TEP) dynamics in relation to trophic and hydrological conditions in the NW Mediterranean Sea. *Mar Ecol-Prog Ser* **262**: 97–109.

Benner R & Strom M (1993) A critical evaluation of the analytical blank associated with DOC measurements by high-temperature catalytic oxidation. *Mar Chem* **41**: 153–160.

Beyenal H, Lewandowski Z & Harkin G (2004) Quantifying biofilm structure: facts and fiction. *Biofouling* **20**: 1–23.

Bond TC, Streets DG, Yarber KF, Nelson SM, Woo JH & Klimont Z (2004) A technology-based global inventory of black and organic carbon emissions from combustion. *J Geophys Res-Atmos* **109**: D14203, DOI: 14210.11029/12003JD003697.

Bongiorni L, Armeni M, Corinaldesi C, Dell'Anno A, Pusceddu A & Danovaro R (2007) Viruses, prokaryotes and biochemical composition of organic matter in different types of mucilage aggregates. *Aquat Microb Ecol* **49**: 15–23.

Bowman JP, McCammon SA, Brown JL & McMeekin TA (1998) *Glaciecola punicea* gen. nov., sp. nov. and *Glaciecola pallidula* gen. nov., sp. nov.: psychrophilic bacteria from Antarctic sea-ice habitats. *Int J Syst Bacteriol* **48**: 1213–1222.

Brakstad OG, Nonstad I, Faksness L & Brandvik PJ (2008) Responses of microbial communities in Arctic sea ice after contamination by crude petroleum oil. *Microb Ecol* **55**: 540–552.

Brussaard CPD, Kuipers B & Veldhuis MJW (2005) A mesocosm study of *Phaeocystis globosa* population dynamics I. Regulatory role of viruses in bloom control. *Harmful Algae* **4**: 859–874.

Busscher H, Dijkstra R, Langwothy D, Collias D, Bjorkquist D, Michell M & Van der Mei H (2008) Interaction forces between waterborne bacteria and activated carbon particles. *J Colloid Interf Sci* **322**: 351–357.

Cochran PK, Kellogg CA & Paul JH (1998) Prophage induction of indigenous marine lysogenic bacteria by environmental pollutants. *Mar Ecol-Prog Ser* **164**: 125–133.

Cornelissen G, Gustafsson O, Bucheli TD, Jonker MTO, Koelmans AA & Van Noort PCM (2005) Extensive sorption of organic compounds to black carbon, coal, and kerogen in sediments and soils: mechanisms and consequences for distribution. *Environ Sci Technol* **39**: 6881–6895.

Dittmar T (2008) The molecular level determination of black carbon in marine dissolved organic matter. *Org Chem* **39**: 396–407.

Ducklow HW (2000) Bacterial production and biomass in the oceans. *Microbial Ecology of the Oceans* (Kirchman DL, ed), pp. 85–120. Wiley-Liss, New York.

Flores-Cervantes DX, Plata DL, MacFarlane JK, Reddy CM & Gschwend PM (2009) Black carbon in marine particulate organic carbon: inputs and cycling of highly recalcitrant organic carbon in the Gulf of Maine. *Mar Chem* **113**: 172–181.

Forbes MS, Raison RJ & Skjemstad JO (2006) Formation, transformation and transport of black carbon (charcoal) in terrestrial and aquatic ecosystems. *Sci Total Environ* **370**: 190–206.

Goldberg ED (1985) *Black Carbon in the Environment*. John Wiley, New York.

Green SJ (2006) A Guide to Denaturing Gradient Gel Electrophoresis. Available at http://ddgehelp.blogspot.com/

Grossart HP, Kiorboe T, Tang K, Allgaier M, Yam EM & Ploug H (2006) Interactions between marine snow and heterotrophic bacteria: aggregate formation and microbial dynamics. *Aquat Microb Ecol* **42**: 19–26.

Guieu C, Roy-Barman M, Leblond N *et al.* (2005) Vertical particle flux in the northeast Atlantic Ocean (POMME experiment). *J Geophys Res Oceans* **110**: C07S18, DOI: 10.1029/2004JC00 2672.

Halloway CF & Cowen JP (1997) Development of a scanning confocal laser microscopic technique to examine the structure and composition of marine snow. *Limnol Oceanogr* **42**: 1340–1352.

Hammes K, Schmidt MW, Smernik R *et al.* (2007) Comparison of quantification methods to measure fire-derived (black/elemental) carbon in soils and sediments using reference materials from soil, water, sediment and the atmosphere. *Global Biogeochem Cy* **21**: GB3016, DOI: 3010.1029/2006GB002914.

Hedges JI, Eglinton G, Hatcher PG *et al.* (2000) The molecularly-uncharacterized component of nonliving organic matter in natural environments. *Org Geochem* **31**: 945–958.

Herndl GJ (1988) Ecology of amorphous aggregations (marine snow) in the Northern Adriatic Sea. II. Microbial density and activity in marine snow and its implication to overall pelagic processes. *Mar Ecol-Prog Ser* **48**: 265–275.

Kepkay PE (1994) Particle aggregation and the biological reactivity of colloids. *Mar Ecol-Prog Ser* **109**: 293–304.

Logan BE & Wilkinson DB (1990) Fractal geometry of marine snow and other biological aggregates. *Limnol Oceanogr* **35**: 130–136.

Luef B, Aspetsberger F, Hein T, Huber F & Peduzzi P (2007) Impact of hydrology on free-living and particle-associated microorganisms in a river floodplain system (Danube, Austria). *Freshwater Biol* **52**: 1043–1057.

Luef B, Neu TR & Peduzzi P (2009a) Imaging and quantifying virus fluorescence signals on aquatic aggregates: a new method and its implication for aquatic microbial ecology. *FEMS Microbiol Ecol* **68**: 372–380.

Luef B, Neu TR, Zweimüller I & Peduzzi P (2009b) Structure and composition of aggregates in two large Europen rivers, based on confocal laser scanning microscopy and image and statistical analysis. *Appl Environ Microb* **18**: 5952–5962.

Malits A & Weinbauer MG (2009) Effect of turbulence and viruses on prokaryotic cell size, production and diversity. *Aquat Microb Ecol* **54**: 243–254.

Mannino A & Harvey HR (2004) Black carbon in estuarine and coastal ocean dissolved organic matter. *Limnol Oceanogr* **49**: 735–740.

Mari X, Rassoulzadegan F, Brussaard CPD & Wassmann P (2005) Dynamics of transparent exopolymeric particles (TEP) production by *Phaeocystis globosa* under N- or P-limitation: a controlling factor of the retention/export balance. *Harmful Algae* **4**: 895–914.

Mari X, Kerros ME & Weinbauer MG (2007) Virus attachment to transparent exopolymeric particles along trophic gradients in the southwestern lagoon of New Caledonia. *Appl Environ Microb* **73**: 5245–5252.

Masiello CA (2004) New directions in black carbon organic geochemistry. *Mar Chem* **92**: 201–213.

Masiello CA & Druffel ERM (1998) Black carbon in deep-sea sediments. *Science* **280**: 1911–1913.

Mostajir M, Dolan JR & Rassoulzadegan F (1995) Seasonal variations of pico- and nano-detrital particles (DAPI Yellow Particles, DYP) in the Ligurian Sea (NW Mediterranean). *Aquat Microb Ecol* **9**: 267–277.

Nagata T (2008) Organic matter–bacteria interactions in seawater. *Microbial Ecology of the Oceans* (Kirchman DL, ed), pp. 207–241. Wiley-Liss, New York.

Neu T, Woelfl S & Lawrence JR (2004) Three-dimensional differentiation of photo-autotrophic biofilm constituents by multi-channel laser scanning microscopy (single-photon and two-photon excitation). *J Microbiol Meth* **56**: 161–172.

Noble RT & Fuhrman JA (1998) Use of SYBR Green I for rapid epifluorescence counts of marine viruses and bacteria. *Aquat Microb Ecol* **14**: 113–118.

Novakov T, Andreae MO, Gabriel R, Kirchstetter TW, Mayol-Bracero OL & Ramanathan V (2000) Origin of carbonaceous aerosols over the tropical Indian Ocean: biomass burning or fossil fuels? *Geophys Res Lett* **27**: 4061–4064.

Peduzzi P & Luef B (2008) Viruses, bacteria and suspended particles in a backwater and main channel site of the Danube (Austria). *Aquat Sci* **70**: 186–194.

Peduzzi P & Weinbauer MG (1993) Effect of concentrating the virus-rich 2–200-nm size fraction of seawater on the formation of algal floes (marine snow). *Limnol Oceanogr* **38**: 1562–1565.

Proctor LM & Fuhrman JA (1991) Roles of viral-infection in organic particle-flux. *Mar Ecol-Prog Ser* **69**: 133–142.

Ramanathan V & Carmichael G (2008) Global and regional climate changes due to black carbon. *Nat Geosci* **1**: 221–227.

Riemann L & Grossart HP (2008) Elevated lytic phage production as a consequence of particle colonization by a marine *Flavobacterium* (*Cellulophaga* sp.). *Microb Ecol* **56**: 505–512.

Samo T, Malfatti F & Azam F (2008) A new class of transparent organic particles in seawater visualized by a novel fluorescence approach. *Aquat Microb Ecol* **53**: 307–321.

Sandradewi J, Prevot ASH, Szidat S *et al.* (2008) Using aerosol light absorption measurements for the quantitative determination of wood burning and traffic emission contributions to particulate matter. *Environ Sci Technol* **42**: 3316–3323.

Schäfer H & Muyzer G (2001) Denaturing gradient gel electrophoresis in marine microbial ecology. *Methods in Microbiology*, *Vol. 30* (Paul J, ed), pp. 425–468. Academic Press, London.

Schmidt MWI & Noack AG (2000) Black carbon in soils and sediments: analysis, distribution, implications, and current challenges. *Global Biogeochem Cy* **14**: 777–793.

Simon M, Grossart HP, Schweitzer B & Ploug H (2002) Microbial ecology of organic aggregates in aquatic ecosystems. *Aquat Microb Ecol* **28**: 175–211.

Slowik JG, Cross ES, Han J-H *et al.* (2007) Measurements of morphology changes of fractal soot particles using coating and denuding experiments: implications for optical absorption and atmospheric lifetime. *Aerosol Sci Tech* **41**: 734–750.

Smith DC, Simon M, Alldredge AL & Azam F (1992) Intense hydrolytic enzyme activity on marine aggregates and implications for rapid particle dissolution. *Nature* **359**: 139–142.

Suttle CA & Chen F (1992) Mechanisms and rates of decay of marine viruses in seawater. *Appl Environ Microb* **58**: 3751–3729.

Van Trappen S, Tan T, Yang J, Mergaert J & Swings J (2004) *Glaciecola polaris* sp. nov., a novel budding and prosthecate bacterium from the Arctic Ocean, and emended description of the genus *Glaciecola*. *Int J Syst Evol Micr* **54**: 1765–1771.

Verdugo P, Alldredge AL, Azam F, Kirchman D, Passow U & Santschi PH (2004) The oceanic gel phase: a bridge in the DOM–POM continuum. *Mar Chem* **92**: 67–85.

Weinbauer MG (2004) Ecology of prokaryotic viruses. *FEMS Microbiol Rev* **28**: 127–181.

Weinbauer MG, Bettarel Y, Cattaneo R, Luef B, Maier C, Motegi C, Peduzzi P & Mari X (2009) Viral ecology of organic and inorganic particles in aquatic systems: avenues for further research. *Aquat Microb Ecol* **57**: 321–341.

Wilhelm SW & Suttle CA (1999) Viruses and nutrient cycles in the sea. *Bioscience* **49**: 781–788.

Winter C, Moeseneder MM & Herndl GJ (2001) Impact of UV radiation on bacterioplankton community composition. *Appl Environ Microb* **67**: 665–672.

Yentsch CS & Yentsch CM (2008) Single cell analysis in biological oceanography and its evolutionary implications. *J Plankton Res* **30**: 107–117.